Green's Function Calculations of Light Nuclei

Zhonghao Sun, Qiang Wu and Furong Xu

School of Physics, Peking University, Beijing 100871, China

Abstract

An influence of short-range correlations in nuclei is investigated with realistic nuclear force. The nucleon-nucleon interaction is renormalized with $V_{\text{low-}k}$ technique and applied to Green's function calculations. The Dyson equation is reformulated using algebraic diagrammatic constructions. We also analyze the ^{4}He binding energy calculated with chiral and CD-Bonn potentials. The properties of Green's function with realistic nuclear forces are also discussed.

Keywords: *Green's function, ab initio calculations, realistic nuclear forces*

1 Introduction

A recent research on theoretical descriptions of nuclear structure has shown that correlations beyond Hartree–Fock (HF) play a significant role. High-resolution nucleon knockout reaction $(e, e'p)$ experiments indicate a probability of a dilution phenomenon in particle occupancy around the Fermi surface. The HF approach is a mean-field method in which the ground state of the system is described with a single Slater determinant and particles occupy only the orbitals below the Fermi surface. Many attempts to account for correlations beyond HF have been made, such as the Jastrow method, configuration interaction methods including the random phase approximation (RPA), the many-body perturbation theory (MBPT), the Bruckner Hartree–Fock (BHF), and the Green's function method.

A development of modern nuclear forces makes it possible to investigate nuclear structure from first principles and perform microscopic calculations with realistic nuclear forces [1]. Although we already have many theoretical methods to study exotic nuclear structures, such as the projected shell model [2] and other phenomenological models [3–6], a microscopic description of nucleus is of great importance for studying fundamental problems in nuclear structure and nuclear forces. The nature of the internucleon force is determined by symmetries of the two-nucleon system; the parameters such as coupling constants and other physical parameters, are fitted to reproduce low-energy phase shifts. Usually, however, realistic nuclear forces cannot be exploited directly in nuclear structure calculations because of their strong short-range repulsive nature. Various methods have been tried to make realistic forces better adjusted for many-body calculations, such as the energy-dependent Bloch–Horowitz method, the

Proceedings of the International Conference 'Nuclear Theory in the Supercomputing Era — 2016' (NTSE-2016), Khabarovsk, Russia, September 19–23, 2016. Eds. A. M. Shirokov and A. I. Mazur. Pacific National University, Khabarovsk, Russia, 2018, p. 52.

http://www.ntse-2016.khb.ru/Proc/Xu.pdf.

Lee–Suzuki transformation [7], the unitary model operator approach (UMOA) [8], and the G-matrix method. In the present study we use realistic nuclear forces for the Green's function calculation of ^{4}He. The difference between the calculations with the CD-Bonn and chiral nuclear N^{3}LO forces is discussed herein.

2 Green's function method

Ab initio self-consistent calculations within the Green's function method have made a great progress since the late 1990s [9]. A brief review of the Green's function theory for many-body systems follows.

Suppose that one has the ground state of a N-particle system, $|\Phi_0\rangle$. The one-particle Green's function is defined as

$$S_{\alpha\beta}(t_1 - t_2) = \langle\Phi_0|\, T\Big[a_\alpha(t_2)a^\dagger_\beta(t_1)\Big]|\Phi_0\rangle, \tag{1}$$

where T is the time ordering operator and $a_\alpha(t)$ is an operator in the Heisenberg picture:

$$a_\alpha(t) = \exp(iHt)\, a_\alpha \exp(-iHt). \tag{2}$$

The single-particle propagator can be written as

$$G_{\alpha\beta}(t_1 - t_2) = \begin{cases} \langle\Phi_0|a_\alpha e^{i(\hat{H}-E_0)(t_1-t_2)}a^\dagger_\beta|\Phi_0\rangle, & t_1 \geq t_2 \\ -\langle\Phi_0|a^\dagger_\beta e^{-i(\hat{H}-E_0)(t_1-t_2)}a_\alpha|\Phi_0\rangle, & t_1 < t_2 \end{cases} \tag{3}$$

One can calculate an expectation value of a single-particle operator by the single-particle propagator,

$$\langle n_\alpha\rangle = -\lim_{t\to+0} G_{\alpha\beta}(t). \tag{4}$$

We use an energy representation of the Green's function $G_{\alpha\beta}(\omega)$ which is the Fourier transformation of $G_{\alpha\beta}(t)$. If we choose the Hartree–Fock basis as a starting point, the Green's function is given by the Dyson equation

$$G_{\alpha\beta}(\omega) = G^{HF}_{\alpha\beta}(\omega) + G^{HF}_{\alpha\gamma_1}(\omega)\,\Sigma_{\gamma_1\gamma_2}(\omega)\,G_{\gamma_2\beta}(\omega) \tag{5}$$

with

$$G^{HF}_{\alpha\beta} = \left[\frac{\Theta(\alpha - F)}{\omega - \epsilon_\alpha + i\eta} + \frac{\Theta(F - \alpha)}{\omega - \epsilon_\alpha - i\eta}\right]\delta_{\alpha\beta}, \tag{6}$$

where G^{HF} is a free Green's function built with Hartree–Fock single-particle energies, and the self-energies $\Sigma(\omega)$ are defined as sums of all one-particle irreducible diagrams (which account for all corrections from other particles [10]). In self-consistent Green's function calculations, the self-energies constructed using fully dressed Green's functions, are defined as

$$\Sigma(\omega)_{ab} = \frac{1}{2}\sum_{\gamma\delta\mu}\int\frac{d\omega_1}{2\pi i}\int\frac{d\omega_2}{2\pi i}\,\langle a\delta|V|\gamma\mu\rangle\langle\gamma\mu|V|b\delta\rangle\, g_\gamma(\omega - \omega_1 + \omega_2)\, g_\delta(\omega_1)\, g_\mu(\omega_2). \tag{7}$$

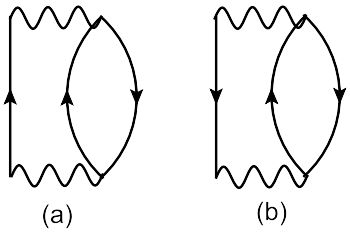

Figure 1: Second order self-energy: a) $2p1h$ and b) $2h1p$ contributions. The wavy line represents the interaction vertex and the solid line is the Green's function.

In the Lehmann representation, the Green's function can be written as

$$\begin{aligned} G_{\alpha\beta}(\omega) &= \int d(t-t')\, e^{i\omega(t-t')} G(t,t') \\ &= \sum_n \frac{\langle\Phi_0|c_\alpha|\Phi_n^{N+1}\rangle\langle\Phi_n^{N+1}|c_\beta^\dagger|\Phi_0\rangle}{\omega + E_0^N - E_n^{N+1} + i\eta} + \sum_m \frac{\langle\Phi_0|c_\alpha^\dagger|\Phi_m^{N-1}\rangle\langle\Phi_m^{N-1}|c_\beta|\Phi_0\rangle}{\omega + E_0^{N-1} - E_0^N - i\eta} \\ &= \sum_n \frac{X_\alpha^n X_\beta^{n*}}{\omega - \omega^+ + i\eta} + \sum_m \frac{X_\alpha^m X_\beta^{m*}}{\omega - \omega^- - i\eta}. \end{aligned} \tag{8}$$

The first term includes a spectroscopic factor indicating the transition from $(A+1)$ to A, and the second term corresponds to the transition from A to $A-1$. The inner structure of the self-energy contains all one-body irreducible diagrams and cannot be calculated exactly; the self-energy is calculated perturbatively using the HF propagator (see Fig. 1). Hereon the Dyson equation can be solved.

The expectation values of single-particle operators can be calculated as

$$\langle\Psi_0|\hat{O}|\Psi_0\rangle = \int_C \frac{d\omega}{2\pi i} \sum_{\alpha\beta} \langle\alpha|\hat{O}|\beta\rangle G_{\alpha\beta}(\omega), \tag{9}$$

where the integration contour encompasses all poles of the Green's function below the Fermi surface (Fig. 2). The particle number conservation is not guaranteed since the self-energy is not calculated with the fully-dressed Green's function.

We calculate the self-energy to the second order and use the algebraic diagrammatic construction (ADC) method to transform the Dyson equation to an eigenvalue problem (details can be found in Ref. [11]),

$$\begin{pmatrix} H_0 & a^T & A^T \\ a & e & 0 \\ A & 0 & E \end{pmatrix} \begin{pmatrix} X \\ X_P \\ X_Q \end{pmatrix} = \omega_n \begin{pmatrix} X \\ X_P \\ X_Q \end{pmatrix}, \tag{10}$$

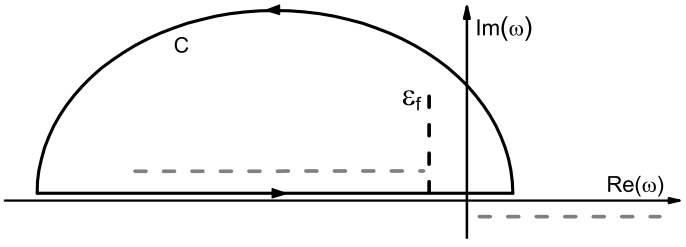

Figure 2: Integration contour for one-body operators wraps the upper half plain encompassing all poles below the Fermi surface ε_f.

where H_0 is the diagonal matrix of Hartree–Fock energies, a is the coupling between single particles,

$$a_{i\alpha} = \langle \alpha h | V | p_1 p_2 \rangle, \tag{11}$$

P is the space spanned by all $2p1h$ states $|p_1 p_2 h\rangle_i$, and A is the coupling to the Q space spanned with all $2h1p$ states $|h_1 h_2 p\rangle_j$,

$$A_{j\alpha} = \langle \alpha p | V | h_1 h_2 \rangle. \tag{12}$$

Respectively, $e = \mathrm{diag}\{e_i^{(p_1,p_2,h)}\}$ and $E = \mathrm{diag}\{e_i^{(h_1,h_2,p)}\}$ are the unperturbed energies in the P and Q spaces. By solving the secular equation (10), one obtains the pole ω_n and corresponding spectroscopic amplitudes X^n defined in Eq. (8)

3 Renormalization of bare nuclear forces

Since 1980s, several modern nuclear forces have been developed based on the fundamental symmetries of nuclear interaction. The local potential Argonne V_{18} [12] is established with all two-body operators that obey the symmetries of angular momentum, parity, and isospin. The parameters are fitted to reproduce low-energy phase shifts and the deuteron binding energy. The CD-Bonn potential [13] is defined in the momentum space and based on the one-boson-exchange mechanism. Chiral interactions are built upon the chiral symmetry breaking of low-energy QCD [14,15]. The soft potential JISP is based on the inverse scattering method [16,17]. All realistic nuclear forces have a similar long-range behavior as they are fitted to low-energy phase shifts (typically up to 350 MeV). The short-range parts of nuclear forces can be however different. A nuclear system is typically dominated by the long-range and intermediate-range parts of nuclear forces. However the couplings between different energy scales of the nuclear force need to be treated properly in order to preserve the symmetries and favour a better perturbation behavior in the system. Some bare forces can be considered as already renormalized [18] and therefore can be directly applied to nuclear structure calculations.

Advanced computer resources make it possible to use bare NN forces in *ab initio* calculations within large model spaces. However the computational burden is remarkably reduced by using renormalization procedures without losing the low-energy physics. Several renormalizing techniques are available. The G-matrix [19,20] sums up the ladder diagrams to infinite orders. The similarity renormalization group (SRG) [21] uses a series of similarity transformations to reduce off-diagonal matrix elements that are responsible for the coupling between the low-energy and high-energy components of nuclear forces. The unitary correlation operator method (UCOM) [22,23] introduces short-range central and tensor correlations into the uncorrelated many-body states by a unitary transformation. The $V_{\text{low-}k}$ approach uses the Lee–Suzuki transformation to decouple the high and low momenta in nuclear forces. By utilizing the similarity transformation, the effective interaction can be decoupled into low- and high-momentum parts thus leading to a faster convergence of calculations. However, the reduction of the model space always generates many-body forces originating from the high-momentum contributions of nuclear force. It has been found that the effects of induced many-body forces are dependent on the model space cutoff. One may find an optimal truncation to neglect the many-body forces. In the present study,

we use the N^{3}LO and CD-Bonn forces. The NN potential is renormalized with the Okamoto–Lee–Suzuki transformation in momentum space [24].

Let H be a full Hamiltonian H with a set of eigenvalues E_k and eigenvectors $|k\rangle$,

$$H|k\rangle = E_k|k\rangle. \tag{13}$$

In practice, H is the Hamiltonian of a certain channel in momentum space or center-of-mass harmonic oscillator basis. The main purpose is to choose a model space P spanned with d vectors $|\alpha_P\rangle$ and the complementary space Q spanned by $|\alpha_Q\rangle$, $P+Q=1$. We seek for a unitary transformation $\mathcal{H} = e^{-\omega}He^{\omega}$ resulting in zero coupling between P and Q spaces, i. e.,

$$Qe^{-\omega}He^{\omega}P = 0. \tag{14}$$

Equation (14) is the decoupling condition; the transformation operator ω is known as a correlation operator which is determined by solving Eq. (14). According to the definition of ω that recovers the Q-space component from the projected wave function, one has

$$P\omega P = Q\omega Q = P\omega Q = 0, \qquad \omega^2 = 0, \tag{15}$$

and a linear form of the transformation is $e^{\omega} = 1+\omega$. Due to the decoupling equation, the effective low-energy interaction which reproduces the d states of the full Hamiltonian, can be written as

$$\begin{aligned} P\mathcal{H}P &= E_k P|k\rangle, \\ \omega P|k\rangle &= Q|k\rangle. \end{aligned} \tag{16}$$

To obtain ω explicitly, one can use

$$\langle\alpha_Q|k\rangle = \sum_{\alpha_P}\langle\alpha_Q|\omega|\alpha_P\rangle\langle\alpha_P|k\rangle. \tag{17}$$

One can find that ω is just a wave operator and corresponds to infinite order corrections to the projected wave function in perturbation. In matrix form, one can rewrite ω in terms of vector components generated by a diagonalization of the full Hamiltonian,

$$\langle\alpha_Q|\omega|\alpha_P\rangle = \sum_{k\in\mathcal{K}}\langle\alpha_Q|k\rangle\langle\tilde{k}|\alpha_P\rangle, \tag{18}$$

where $\langle\tilde{k}|\alpha_P\rangle$ is the biorthogonal vector to a projected P-space state vector, i. e., $\sum_{\alpha_P}\langle\tilde{k}|\alpha_P\rangle\langle\alpha_P|k'\rangle = \delta_{kk'}$. Once the transformation operator ω is constructed, a Hermitian effective Hamiltonian can be found as [24]

$$H_{eff} = \frac{P+P\omega^{\dagger}Q}{\sqrt{P(1+\omega^{\dagger}\omega)P}}H\frac{Q\omega P+P}{\sqrt{P(1+\omega^{\dagger}\omega)P}}. \tag{19}$$

The unitary transformation is not unique. A detailed discussion can be found in Ref. [25].

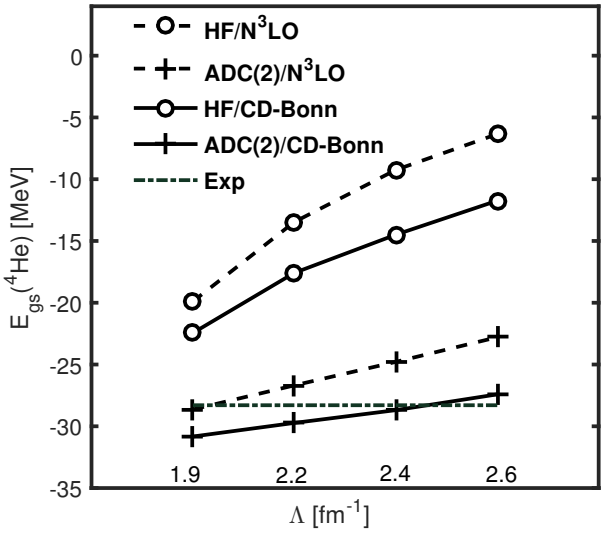

Figure 3: Hartree–Fock and Green's function calculations of ^{4}He with N3LO and CD-Bonn NN potentials. The Green's function approach utilizes the ADC method for solving the Dyson equation.

4 Calculations and discussion

In order to investigate high-momentum contributions in the N^{3}LO and CD-Bonn NN potentials, we renormalize the bare forces with $V_{\text{low-}k}$ procedure with the momentum space cutoff Λ varying from 1.9 fm^{-1} to 2.6 fm^{-1}. The N3LO interaction should be accompanied by a generic three-body force which contains counter-terms in renormalization of the two-body part. An additional three-body force originates due to the $V_{\text{low-}k}$ procedure used for the further reduction of model space. In our calculations the induced three-body force is neglected. However, as we increase the momentum cutoff, the Hartree–Fock calculations of ^{4}He result in decrease of the binding energy (Fig. 3). This result stems from the fact that the short-range repulsive part of the nuclear forces becames stronger. As discussed above, by including configuration interaction in the Green's function, we can obtain the correct binding energy. We see that the Green's function calculations provide a much better convergence than the HF calculations. Figure 4 displays the convergence of HF and Green's function calculations with respect to $\hbar\omega$. A good convergence is obtained in both the HF and Green's function methods, but the Green's function provides a much better binding energy as compared with the experimental data. This result implies that high-order contributions which are beyond the HF are important.

5 Conclusion

Starting with realistic nucleon-nucleon interactions and modern renormalization technique, we performed *ab initio* calculations of ^{4}He with the Green's function method. High-order correlations can be well described by including the $2p1h$ and $2h1p$ configurations. In order to consider short-range correlations, one has to include higher-order terms in the self-energy calculations. In addition, the induced three-body force has to be treated exactly.

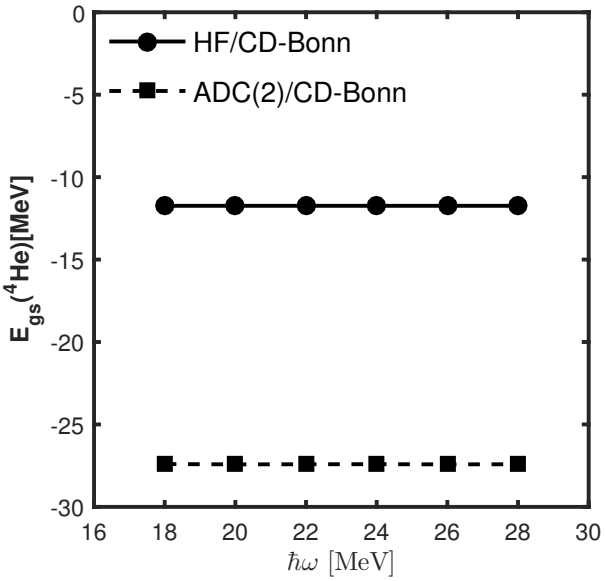

Figure 4: Hartree–Fock and Green's function calculations of ^{4}He with CD-Bonn NN potential with various $\hbar\omega$ values and $\Lambda = 2.6$ fm^{-1}.

References

[1] X. B. Wang and G. X. Dong, Sci. China Phys. Mech. Astron. **58**(10), 102001 (2015).

[2] Y. X. Liu, S. Y. Yu and C. W. Shen, Sci. China Phys. Mech. Astron. **58**(1), 012001 (2015).

[3] Q. H. Mo, M. Liu, L. C. Cheng, N. Wang, Sci. China Phys. Mech. Astron. **58**(8), 082001 (2015).

[4] X. H. Fan, J. M. Dong and W. Zuo, Sci. China Phys. Mech. Astron. **58**(6), 062002 (2015).

[5] G. X. Dong, X. B. Wang and S. Y. Yu, Sci. China Phys. Mech. Astron. **58**(11), 112004 (2015).

[6] K. P. Xie, W. Y. Ke, W. Y. Liang, X. M. Fu, C. F. Jiao, J. C. Pei and F. R. Xu, Sci. China Phys. Mech. Astron. **57**(2), 189 (2014).

[7] P. Navrátil, J. P. Vary and B. R. Barrett, Phys. Rev. C **62**, 054311 (2000).

[8] S. Fujii, R. Okamoto and K. Suzuki, J. Phys. Conf. Ser. **20**, 83 (2005).

[9] A. Carbone, A. Cipollone, C. Barbieri, A. Rios and A. Polls, Phys. Rev. C **88**, 054326 (2013).

[10] K. Amir-Azimi-Nili, H. Müther, L. D. Skouras and A. Polls, Nucl. Phys. A **604**, 245 (1996).

[11] H. Müther and L.D. Skouras, Nucl. Phys. A **555**, 541 (1993).

[12] R. B. Wiringa, V. G. J. Stoks and R. Schiavilla, Phys. Rev. C **51**, 38 (1995).

[13] R. Machleidt, Phys. Rev. C **63**, 024001 (2001).

[14] D. R. Entem and R. Machleidt, Phys. Rev. C **68**, 041001 (2003).

[15] R. Machleidt and D. Entem, Phys. Rep. **503**, 1 (2011).

[16] A. M. Shirokov, A. I. Mazur, S. A. Zaytsev, J. P. Vary and T. A. Weber, Phys. Rev. C **70**, 044005 (2004).

[17] A. M. Shirokov, J. P. Vary, A. I. Mazur, S. A. Zaytsev and T. A. Weber, Phys. Lett. B **621**, 96 (2005).

[18] I. Stetcu, J. Rotureau, B. R. Barrett and U. van Kolck, J. Phys. G **37**, 064033 (2010).

[19] M. Borromeo, D. Bonatsos, H. Müther and A. Polls, Nucl. Phys. A **539**, 189 (1992).

[20] M. Hjorth-Jensen, T. T. Kuo and E. Osnes, Phys. Rep. **261**, 125 (1995).

[21] S. K. Bogner, R. J. Furnstahl and R. J. Perry, Phys. Rev. C **75**, 061001 (2007).

[22] R. Roth, H. Hergert, P. Papakonstantinou, T. Neff and H. Feldmeier, Phys. Rev. C **72**, 034002 (2005).

[23] R. Roth, T. Neff and H. Feldmeier, Prog. Part. Nucl. Phys., **65**, 50 (2010).

[24] K. Suzuki and R. Okamoto, Progr. Theor. Phys. **70**, 439 (1983).

[25] J. D. Holt, T. T. S. Kuo and G. E. Brown, Phys. Rev. C **69**, 034329 (2004).